




# Single- and double-ionization processes of antiproton-helium and antiproton–molecular hydrogen collisions in the keV energy range

C. C. Jia <sup>1,2</sup> T. Kirchner <sup>3</sup> J. W. Gao,<sup>4</sup> Y. Wu,<sup>1</sup> J. G. Wang,<sup>1</sup> and N. Sisourat <sup>2,\*</sup>

<sup>1</sup>Key Laboratory of Computational Physics, Institute of Applied Physics and Computational Mathematics, Beijing 100088, China

<sup>2</sup>Laboratoire de Chimie Physique-Matière et Rayonnement, Sorbonne Université, CNRS, 75005 Paris, France

<sup>3</sup>Department of Physics and Astronomy, York University, Toronto, Ontario, Canada M3J 1P3

<sup>4</sup>School of Physics, Hangzhou Normal University, Hangzhou 311121, China



(Received 11 October 2022; accepted 5 January 2023; published 13 January 2023)

We report on an *ab initio* model to describe single- and double-ionization processes in antiproton collisions with atoms and molecules. Our model is based on a fully correlated close-coupling approach and a Dyson orbital analysis. Furthermore, we employ the concept of a correlation integral in order to quantify and gain insights into the effects of electronic correlation on the ionization processes. Our model is applied to the prototype antiproton-helium and antiproton–molecular hydrogen collision systems in the keV energy range.

DOI: [10.1103/PhysRevA.107.012808](https://doi.org/10.1103/PhysRevA.107.012808)

## I. INTRODUCTION

Collisions between antiprotons and atoms and molecules have attracted a renewed attention in the last decade [1,2] for several reasons. From a fundamental point of view, these collisions are central to understanding the physics of antiparticles [3]. In more applied perspectives, processes occurring in a single antiproton collision are responsible for the slowing down and thus energy deposition of the ions into solids, which is relevant in material science [4] and radiation therapy [5].

The theoretical description of the electronic processes occurring in antiproton-atom and antiproton-molecule collisions is, in general, challenging. Single and multiple ionization are important processes but dealing with continuum states remains difficult in most practical cases. Furthermore, electronic correlation is a driving force of these processes. To date, there are only a few works published in which a fully active electron description is achieved. A number of approximate methods have become available to deal with electronic correlation and many-electron processes (see Ref. [6] and references therein). However, a general and accurate approach is still not available, especially to treat molecular targets.

In this paper, we propose a model based on a fully correlated close-coupling approach and a Dyson orbital analysis to describe single- and multiple-ionization processes in antiproton-atom and antiproton-molecule collisions. Furthermore, we employ the concept of a correlation integral to analyze and gain insights into our results. Our approach is tested on antiproton-helium and antiproton–molecular hydrogen collision systems, which are benchmark examples. These systems have been extensively investigated in the past. Previous works on this topic are reviewed in, e.g., Refs. [1,2]. However, the approach is general and thus can, in principle, be employed for any collision systems involving antiprotons.

The paper is structured as follows: In Sec. II, we present our close-coupling approach and the analysis scheme using

Dyson orbitals. We also introduce the concept of a correlation integral and provide the computational details. In Sec. III, we first discuss the case of a helium target and then the molecular hydrogen target system. For both cases, we compare our single- and double-ionization cross sections with previous results. An overall good agreement between the data is shown. These processes are finally analyzed using the correlation integrals. The latter show that the electron-electron correlation has different effects depending on the collision energy, but is qualitatively independent on the target and on its orientation (for the molecular case). The conclusions of this paper are reported in Sec. IV.

## II. METHODS AND COMPUTATIONAL DETAILS

In the present paper, we use the impact parameter method [7–9] in which the relative motion of the nuclei is described by a classical trajectory  $\vec{R}(t)$  while a quantum approach is adopted for the electron dynamics.  $\vec{R}(t)$  is the position vector of the projectile relative to the target described by a straight-line constant velocity trajectory  $\vec{R}(t) = \vec{b} + \vec{v}_p t$ , where  $\vec{b}$  is the impact parameter and  $\vec{v}_p$  is the relative velocity vector between the target and projectile. For a two-electron system, the time-dependent Schrödinger equation (TDSE) describing the dynamics of the electrons is

$$\left[ \hat{H}_{\text{el}} - i \frac{\partial}{\partial t} \right] \Psi(\vec{r}_1, \vec{r}_2, \vec{R}(t)) = 0, \quad (1)$$

where  $\hat{H}_{\text{el}}$  is the electronic Hamiltonian,

$$\hat{H}_{\text{el}} = \sum_{i=1,2} \left( -\frac{1}{2} \nabla_i^2 + \vec{V}_T(\vec{r}_i) + \vec{V}_P(\vec{r}_i^p) \right) + \frac{1}{|\vec{r}_1 - \vec{r}_2|}, \quad (2)$$

and  $\vec{r}_i, \vec{r}_i^p = \vec{r}_i - \vec{R}(t)$  are the position vectors of the electrons with respect to the target and the projectile, respectively.

In our calculations, we solve the time-dependent Schrödinger equation by assuming that the electronic wave function can be expanded using a finite set of basis functions

\*Nicolas.Sisourat@sorbonne-universite.fr

$\chi_k(\{\vec{r}\})$ , with  $\{\vec{r}\} = (\vec{r}_1, \vec{r}_2)$ , i.e., the electronic wave function is approximated by the expansion

$$\Psi(\{\vec{r}\}, \vec{R}(t)) = \sum_{k=1}^N c_k(t) \chi_k(\{\vec{r}\}), \quad (3)$$

where  $\chi_k(\{\vec{r}\})$  are target eigenstates. The latter are obtained by diagonalization of the target electronic Hamiltonian in a given Gaussian basis set. Note that in the case of a molecular target, the Hamiltonian in Eq. (2) and the electronic wave function in Eq. (3) depend on the molecular geometry and the molecular orientation with respect to  $\vec{R}(t)$ .

Substituting the wave function Eq. (3) into Eq. (1) and projecting into each of the target states lead to a set of coupled first-order differential equations for the expansion coefficients, which are written in matrix form as

$$i \frac{d}{dt} \mathbf{c}(t) = \mathbf{S}^{-1}(\vec{b}, \vec{v}, t) \mathbf{M}(\vec{b}, \vec{v}, t) \mathbf{c}(t), \quad (4)$$

where  $\mathbf{c}(t)$  is the column vector of the time-dependent expansion coefficients, and  $\mathbf{S}$ ,  $\mathbf{M}$  are the overlap and coupling matrices, respectively.

The electronic Hamiltonian depends on time due to the classical relative motion of the nuclei  $\vec{R}(t)$ , which depends explicitly on the impact parameter  $\vec{b}$ . For a given collision energy, Eq. (4) is solved using the predictor-corrector Adams-Bashforth-Moulton method for a set of impact parameters. The total cross section for a given electronic process is

$$\sigma_f = 2\pi \int_0^{+\infty} b P_{i \rightarrow f}(b) db, \quad (5)$$

where  $P_{i \rightarrow f}(b)$  is the probability of the transition  $i \rightarrow f$  which reads

$$P_{i \rightarrow f}(b) = \lim_{t \rightarrow \infty} |c_f(t)|^2. \quad (6)$$

Several implementations of the impact parameter method have been proposed. A review of these approaches can be found in, e.g., Ref. [9]. In our calculations, ionization processes are described using a set of target pseudocontinuum states. The latter are only approximations of the true continuum states because of the use of Gaussian functions. In this paper, we develop a model based on Dyson orbitals (hereafter referred to as the Dyson model) to sort the pseudocontinuum states into single- and double-electron continuum states.

A Dyson orbital is defined as

$$\phi_{kj}(\vec{r}) = \int d\vec{r}_2, \dots, d\vec{r}_N \chi_k^{T^+}(\vec{r}_2, \dots, \vec{r}_N) \chi_j^T(\{\vec{r}\}), \quad (7)$$

where the  $\chi_k$  are the cationic ( $T^+$ ) or neutral ( $T$ ) target eigenstates.

The sum (over all bound states  $k$  of  $T^+$ ) of the norms of the Dyson orbitals (SND) for the state  $j$  of  $T$  is defined as

$$\mathcal{D}_j = \sum_k P_{kj} = \sum_k \int d\vec{r} |\phi_{kj}(\vec{r})|^2. \quad (8)$$

The  $\mathcal{D}_j$  represents the probability that one electron in the pseudostate  $j$  is in a bound orbital of the cation. For a two-electron system, using the SND, the distribution of electrons in the pseudostate  $j$  of the neutral target can be grouped into

three classes [10]: (i) Both electrons are in a bound orbital, corresponding to double excitation, which has a probability  $(\mathcal{D}_j)^2$ ; (ii) both electrons are in the continuum, corresponding to double ionization, with a probability  $(1 - \mathcal{D}_j)^2$ ; (iii) one electron is in a bound orbital and the second electron is in the continuum corresponding to single ionization with a probability  $2 \times (\mathcal{D}_j)(1 - \mathcal{D}_j)$ .

Accordingly, the total single-ionization cross sections  $\sigma_{\text{SI}}$  are computed as

$$\sigma_{\text{SI}} = \sum_j^{N_{\text{IP}}} \sigma_j + \sum_j^{N_{\text{DIP}}} 2 \times \mathcal{D}_j (1 - \mathcal{D}_j) \sigma_j. \quad (9)$$

Note that the contribution of the autoionization states to the SI cross sections is small and was neglected in the above equation. The total double-ionization cross sections  $\sigma_{\text{DI}}$  are computed as

$$\sigma_{\text{DI}} = \sum_{j=1}^{N_{\text{DIP}}} (1 - \mathcal{D}_j)^2 \sigma_j, \quad (10)$$

where  $\sigma_j$  is the cross section of the pseudocontinuum state  $j$ .  $N_{\text{IP}}$  and  $N_{\text{DIP}}$  are, respectively, the number of pseudocontinuum states in the energy range between the ionization potential (IP) and double-ionization potential (DIP) and above the DIP. The Dyson model allows us to compute total single- and double-ionization cross sections without considering explicitly the continuum. It can, therefore, be easily implemented in any quantum chemistry packages. However, it cannot provide, for example, differential cross sections. To compute the latter, one would need to project the wave function over model continuum wave functions (see, e.g., Ref. [11] and references therein for a discussion on the different models). Such a model has been applied for antiproton-helium collisions in Ref. [12].

With a view on the single- and double-ionization problem, we denote the probabilities for ionizing 0, 1, and 2 electrons as  $p_0$ ,  $p_1$ , and  $p_2$ , respectively. The average probability for ionizing one electron is defined as

$$p = \frac{1}{2}(p_1 + 2p_2). \quad (11)$$

Furthermore, we introduce the so-called correlation integral  $I_c$  [1] to quantify the effects of the electronic correlation. Following Ref. [13], we have

$$p_0 = (1 - p)^2 + \frac{1}{2}I_c, \quad (12)$$

$$p_1 = 2p(1 - p) - I_c, \quad (13)$$

$$p_2 = p^2 + \frac{1}{2}I_c. \quad (14)$$

From these equations we obtain  $I_c = 2p_0p_2 - \frac{1}{2}p_1^2$ , which we can use to calculate  $I_c$  from the probabilities corresponding to Eqs. (9) and (10) and the normalization condition  $p_0 = 1 - p_1 - p_2$ .

We use the CIPPRES package [14] to do the singly and doubly excited configuration interaction calculations (labeled CISD hereafter). Note that this is a full configuration interaction for the two-electron collision systems considered in this paper. CIPPRES is a plugin for QUANTUM PACKAGE 2.0 (QP2) [15]. The pseudostates are obtained by diagonalization of the electronic Hamiltonian matrix which is built

TABLE I. cc-pVTZ-6kbj;  $c_l$  and  $\zeta_l$  are, respectively, the Gaussian function coefficient and exponent.

Orbital	Total number	No.	$\zeta_l$	$c_l$
S	4	1	234.000000	0.0025870
		2	35.160000	0.0195330
		3	7.989000	0.0909980
		4	2.212000	0.2720500
S	1	1	0.6669000	1.0000000
S	1	1	0.2089000	1.0000000
P	1	1	3.0440000	1.0000000
P	1	1	0.7580000	1.0000000
D	1	1	1.9650000	1.0000000
S	1	1	0.2456452	1.0000000
P	1	1	0.1693411	1.0000000
D	1	1	0.6225575	1.0000000
S	1	1	0.0984957	1.0000000
P	1	1	0.0898939	1.0000000
D	1	1	0.2421608	1.0000000
S	1	1	0.0527254	1.0000000
P	1	1	0.0556109	1.0000000
D	1	1	0.1278396	1.0000000
S	1	1	0.0327748	1.0000000
P	1	1	0.0377660	1.0000000
D	1	1	0.0788350	1.0000000
S	1	1	0.0223274	1.0000000
P	1	1	0.0273116	1.0000000
D	1	1	0.0534281	1.0000000
S	1	1	0.0161822	1.0000000
P	1	1	0.0206659	1.0000000
D	1	1	0.0385827	1.0000000

using Slater determinants of Hartree-Fock (HF) orbitals. In the computations of antiproton-helium collisions, we used the cc-pVTZ-6kbj basis set (see Table I) to do the calculations, and about 4700 configurations are used to describe the pseudostates. Pseudostates with energy up to 5 a.u. are kept in our calculations (i.e., 1800 states). In the computations of antiproton-molecular hydrogen collisions, we used the aug-cc-pVDZ-3kbj basis set (see Table II). About 5250 configurations are used to describe the pseudostates. Pseudostates with energy up to 7 a.u. are kept in our calculations (i.e., 2600 states). Our CISD total single- and double-ionization cross sections are computed by taking the average over three different orthogonal molecular orientations as in Ref. [16]. Previous studies have shown that this is sufficient to provide accurate estimates of the total cross sections [16–18].

### III. RESULTS AND DISCUSSIONS

#### A. Antiproton-helium collisions

In Fig. 1, we first compare the present CISD calculations for the total single-ionization cross sections at collision energies ranging from 1 up to 1000 keV with experimental data measured at CERN by Andersen *et al.* (CERN 90) [19], by Hvelplund *et al.* (CERN 94) [20], by Knudsen *et al.* (CERN 08) [21], and the time-dependent close-coupling (TDCC) theoretical calculation [22] and the finite-element discrete-variable representation (labeled FE-DVR hereafter) results

TABLE II. aug-cc-pVDZ-3kbj;  $c_l$  and  $\zeta_l$  are, respectively, the Gaussian function coefficient and exponent.

Orbital	Total number	No.	$\zeta_l$	$c_l$
S	3	1	13.0100000	0.0196850
		2	1.9620000	0.1379770
		3	0.4446000	0.4781480
S	1	1	0.1220000	1.0000000
S	1	1	0.0297400	1.0000000
P	1	1	0.7270000	1.0000000
P	1	1	0.1410000	1.0000000
S	1	1	0.2456452	1.0000000
P	1	1	0.1693411	1.0000000
D	1	1	0.6225575	1.0000000
S	1	1	0.0984957	1.0000000
P	1	1	0.0898939	1.0000000
D	1	1	0.2421608	1.0000000
S	1	1	0.0527254	1.0000000
P	1	1	0.0556109	1.0000000
D	1	1	0.1278396	1.0000000

[23]. The calculated total SI cross sections increase from low impact energies up to around 60 keV and then decrease at higher energies. Our CISD predictions are above the experimental data in the energy range between 10 and 20 keV. For collision energies in the 25–1000 keV range, the total SI cross sections of CISD are slightly below the experimental and TDCC results, while for collision energies in the 25–200 keV range, the total SI cross sections of CISD are larger than the FE-DVR results.

Figure 2 shows the present CISD total double-ionization cross sections compared with Andersen *et al.* [19] (CERN 90), Hvelplund *et al.* [20] (CERN 94), and Knudsen *et al.* [24] (CERN 09), the TDCC theoretical results [22] and the FE-DVR results [23]. As the SI, the total DI cross sections also increase from lower impact energies up to about 50 keV and

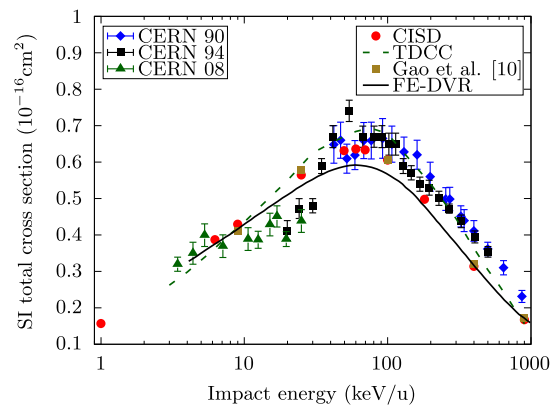


FIG. 1. Total single-ionization cross sections of He by antiproton impact plotted as functions of the impact energy. The present CISD results are compared with the experimental data of Andersen *et al.* (CERN 90) [19], Hvelplund *et al.* (CERN 94) [20], and Knudsen *et al.* (CERN 08) [21]. We also compare our results with the TDCC results [22], the clustering analysis results [10], and the FE-DVR results [23].

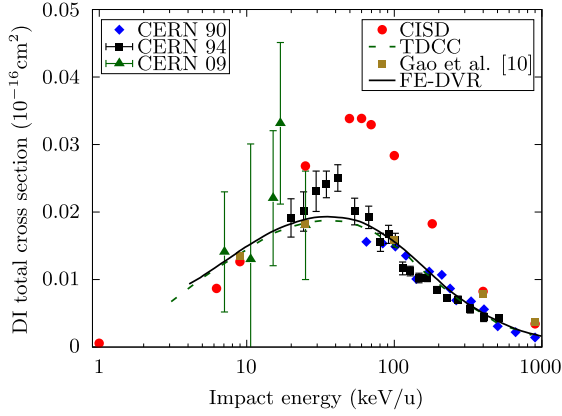


FIG. 2. Total double-ionization cross sections of He by antiproton impact plotted as functions of the impact energy. Experimental data of Andersen *et al.* [19] (CERN 90), Hvelplund *et al.* [20] (CERN 94), and Knudsen *et al.* [24] (CERN 09), and also the theoretical TDCC results [22], the clustering analysis results [10], and the FE-DVR results [23] are compared with the present CISD results.

decrease at higher energies. Our CISD total DI cross sections are in good agreement with the experimental and TDCC data in the collision energy range 1–30 keV. For collision energies larger than 30 keV, the CISD results overestimate the DI cross sections compared to the TDCC, the FE-DVR results, and the experimental data.

Given the challenging task to describe single- and double-ionization processes, the agreement between our results and previous data can be deemed satisfactory.

Now, we focus on the correlation integral  $I_c$ . Figure 3 shows the correlation integral  $I_c$  computed using CISD ionization probabilities as functions of the impact parameter for different collision velocities. We can see that  $I_c$  changes from negative values to positive values as the impact velocity increases. Negative values of  $I_c$  lower the DI processes while positive values enhance them. For  $v_p = 0.2$  a.u., the correlation integral  $I_c$  is always negative. For  $v_p = 1.0$  a.u.,  $I_c$  gets larger at small impact parameter  $b$  but is still negative. For  $v_p = 4.0$  a.u.,  $I_c$  becomes positive. For  $I_c < 0$ , the DI

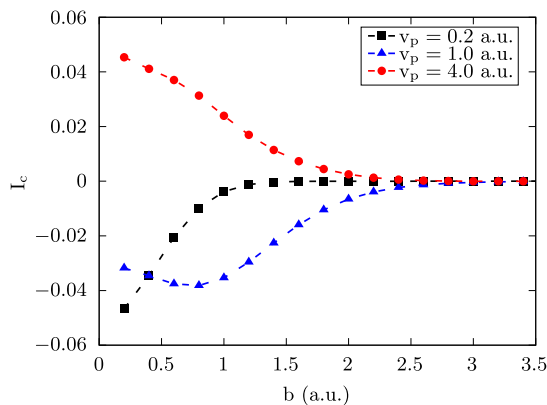


FIG. 3. The correlation integral  $I_c$  is shown for the collision velocities  $v_p = 0.2, 1.0,$  and  $4.0$  a.u. as functions of the impact parameter.

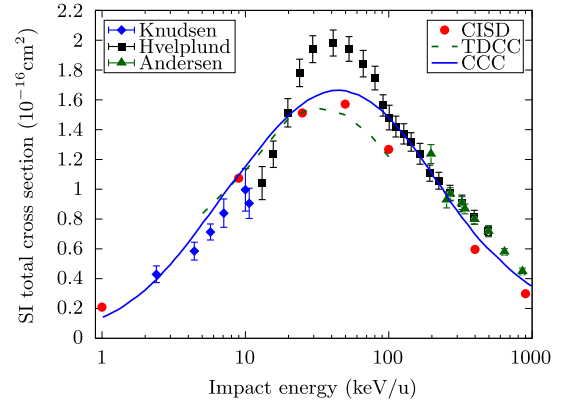


FIG. 4. Total single-ionization cross sections of  $H_2$  by antiproton impact plotted as functions of the impact energy. Present CISD results are compared with the experimental data for nondissociative ionization of Andersen *et al.* [36], Hvelplund *et al.* [20], and Knudsen *et al.* [37], and theoretical TDCC [38] and CCC [39,40] results.

cross sections are decreased possibly because of the electron recapture effect existing in many collision processes [25–28]. For  $I_c > 0$ , the shakeoff [29–31] and knockout [32–34] effects may contribute to the DI processes, thus enhancing their probabilities at high energies.

Note that in Ref. [10], we proposed a method based on a clustering analysis to separate the pseudocontinuum states into single- and double-ionization states. From this analysis, single- and double-ionization cross sections in antiproton-helium collisions were obtained. This approach is accurate for helium as a target, but performs poorly for the molecular hydrogen case (not shown). The results of the present approach are compared to the clustering ones in Figs. 1 and 2, respectively, for the helium case. The single-ionization cross sections obtained with both methods agree with each other. There are some differences in the double-ionization cross sections for energies between 25 and 100 keV. The previous results agree better with other data. However, the present ap-

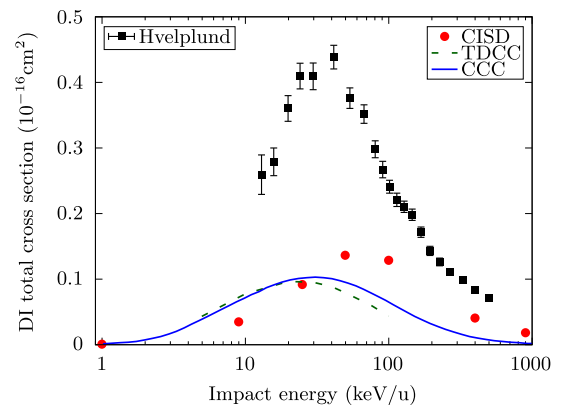


FIG. 5. Total double-ionization cross sections of  $H_2$  by antiproton impact plotted as functions of the impact energy. We compare the present CISD results with the theoretical TDCC [38] and CCC [40] results. The experimental productions of  $H^+$  data of Hvelplund *et al.* [20] are also shown.

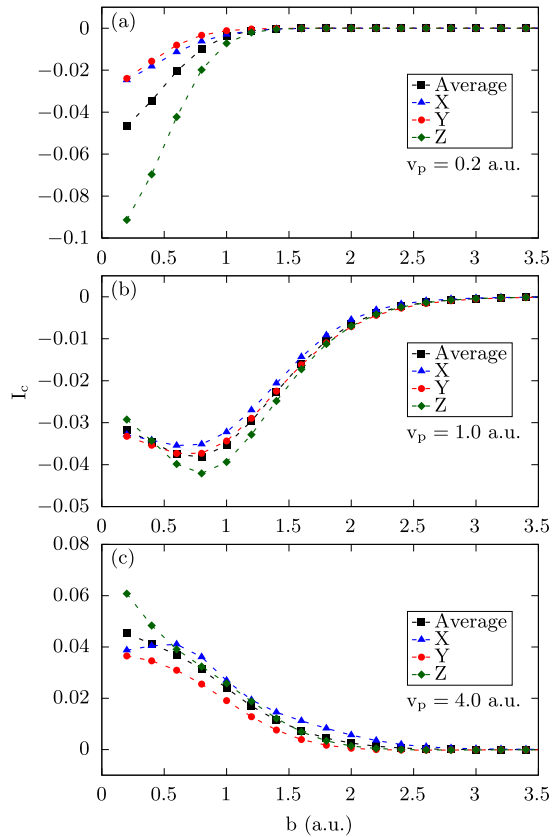


FIG. 6. The correlation integral  $I_c$  of the average and the three orthogonal molecular orientations are shown for the collision velocities  $v_p = 0.2, 1.0,$  and  $4.0$  a.u. plotted as functions of the impact parameter.  $Z$  is the axis along the collision velocity,  $X$  is along the impact parameter, and  $Y$  is the axis perpendicular to the collision plane.

proach is more general since the performance of the clustering analysis is system dependent [35].

### B. Antiproton–molecular hydrogen collisions

The present CISD calculations for the total single-ionization cross sections at collision energies ranging from 1 up to 1000 keV are compared in Fig. 4 with the experimental data of Hvelplund *et al.* [20], Andersen *et al.* [36], and Knudsen *et al.* [37], and the theoretical TDCC [38] and time-dependent convergent close-coupling (CCC) [39,40] results. The cross-section curve exhibits a bell shape. The maximum appears at around 50 keV. Our CISD results are in good agreement with the theoretical TDCC and CCC results and the experimental data, except in the 25–1000 keV range where the CISD theoretical predictions are slightly below the experimental data.

For double ionization in Fig. 5, our CISD results are compared with the experimental data of Hvelplund *et al.* [20] and also the theoretical TDCC [38] and CCC [40] results. Here, the experimental data of Hvelplund *et al.* correspond to the production of  $H^+$  ions. Since single-ionization processes can also lead to the production of  $H^+$  ions, the experimental data represent an upper limit for the double-ionization cross

sections. We can see that the present CISD results show a reasonably good agreement with the TDCC and CCC data in the energy range 1–30 keV, with the exception at energies around 10 keV where the CISD results underestimate the theoretical reference data. In the energy range 30–1000 keV, the CISD results slightly overestimate the total DI cross sections compared to the TDCC and CCC data. The calculated total DI cross sections also increase at lower impact energies and decrease at higher energies with the maximum at energy around 50 keV. Similarly to the antiproton-helium collision system, the total SI cross sections are larger than the DI cross sections. We can see that both the total SI and DI cross sections of antiproton–molecular hydrogen are larger than the total SI and DI cross sections of antiproton-helium, respectively.

The correlation integral  $I_c$  is shown in Fig. 6 for different molecular orientations and collision velocities. We see that for  $v_p = 0.2$  a.u., the correlation integral  $I_c$  is only negative, for  $v_p = 1.0$  a.u.,  $I_c$  still remains negative, while for  $v_p = 4.0$  a.u. the  $I_c$  is positive. This behavior is similar to the antiproton-helium collision case. In addition, we also investigate the effects of molecular orientation on the ionization cross sections and the correlation integral. According to our CISD ionization cross-section results and Fig. 6, there is no significant orientation effect at the higher velocities. At the lowest one, small differences are seen. The weak molecular orientation effect indicates that taking the average over three orthogonal molecular orientations is a reasonable approximation.

## IV. CONCLUSIONS

In this paper, we have theoretically investigated the single- and double-ionization processes of antiproton-helium and antiproton–molecular hydrogen collision systems. The impact parameter method, close-coupling approach, and a Dyson model are employed in our calculations. We computed the corresponding total single- and double-ionization cross sections in the collision energy range 1–1000 keV, which show good overall agreement compared with the experimental and theoretical data.

We also used the concept of a correlation integral  $I_c$  to get further insights into the electronic dynamics. Our results show that the correlation integral changes its sign from negative to positive as the collision velocity increases. Therefore, electronic correlation inhibits double-ionization processes at low impact energies and enhances them at high collision energies. This behavior could be related to electron recapture effects at low collision energies and shakeoff and knockout effects at higher collision energies.

## ACKNOWLEDGMENTS

C.C.J. is supported by a China Scholarship Council (CSC) scholarship within a CSC-SU program. C.C.J., J.W.G., J.G.W., and Y.W. acknowledge the support of the National Natural Science Foundation of China (Grants No. 11934004 and No. 12004350). T.K. acknowledges support from the Natural Sciences and Engineering Research Council of Canada (Grant No. RGPIN-2019-06305).



- [1] T. Kirchner and H. Knudsen, *J. Phys. B: At., Mol. Opt. Phys.* **44**, 122001 (2011).
- [2] T. Kirchner, in *Ion-Atom Collisions: The Few-Body Problem in Dynamic Systems*, edited by M. Schulz (De Gruyter, Berlin, 2019), pp. 35–60.
- [3] S. Jonsell, *Philos. Trans. R. Soc. A* **376**, 20170271 (2018).
- [4] K. Nordlund, M. Hori, and D. Sundholm, *Phys. Rev. A* **106**, 012803 (2022).
- [5] J. Bailey, A. Kadyrov, I. Abdurakhmanov, D. Fursa, and I. Bray, *Phys. Med.* **32**, 1827 (2016).
- [6] H. J. Lüdde, M. Horbatsch, and T. Kirchner, *Phys. Rev. A* **104**, 032813 (2021).
- [7] D. R. Bates and R. McCarroll, *Proc. R. Soc. London, Ser. A* **245**, 175 (1958).
- [8] B. Bransden, M. McDowell, and E. J. Mansky, *Phys. Today* **46**(10), 124 (1993).
- [9] N. Sisourat and A. Dubois, in *Ion-Atom Collisions: The Few-Body Problem in Dynamic Systems*, edited by M. Schulz (Boston: De Gruyter, Berlin, 2019), pp. 157–178.
- [10] J. W. Gao, T. Miteva, Y. Wu, J. G. Wang, A. Dubois, and N. Sisourat, *Phys. Rev. A* **103**, L030803 (2021).
- [11] A. Benedek and R. I. Campeanu, *J. Phys. B: At., Mol. Opt. Phys.* **40**, 1589 (2007).
- [12] I. B. Abdurakhmanov, A. S. Kadyrov, I. Bray, and K. Bartschat, *Phys. Rev. A* **96**, 022702 (2017).
- [13] M. Baxter and T. Kirchner, *Phys. Rev. A* **87**, 062507 (2013).
- [14] N. Sisourat, CIPPRES, [https://github.com/sisourat/qp2\\_plugins\\_nsisourat](https://github.com/sisourat/qp2_plugins_nsisourat).
- [15] Y. Garniron, T. Applencourt, K. Gasperich, A. Benali, A. Ferté, J. Paquier, B. Pradines, R. Assaraf, P. Reinhardt, J. Toulouse, P. Barbaresco, N. Renon, G. David, J.-P. Malrieu, M. Véril, M. Caffarel, P.-F. Loos, E. Giner, and A. Scemama, *J. Chem. Theory Comput.* **15**, 3591 (2019).
- [16] N. Sisourat, I. Pilskog, and A. Dubois, *Phys. Rev. A* **84**, 052722 (2011).
- [17] L. F. Errea, J. D. Gorfinkiel, A. Macías, L. Méndez, and A. Riera, *J. Phys. B: At., Mol. Opt. Phys.* **30**, 3855 (1997).
- [18] J. Caillat, N. Sisourat, A. Dubois, I. Sundvor, and J. P. Hansen, *Phys. Rev. A* **73**, 014701 (2006).
- [19] L. H. Andersen, P. Hvelplund, H. Knudsen, S. P. Møller, J. O. P. Pedersen, S. Tang-Petersen, E. Uggerhøj, K. Elsener, and E. Morenzoni, *Phys. Rev. A* **41**, 6536(R) (1990).
- [20] P. Hvelplund, H. Knudsen, U. Mikkelsen, E. Morenzoni, S. P. Møller, E. Uggerhøj, and T. Worm, *J. Phys. B: At., Mol. Opt. Phys.* **27**, 925 (1994).
- [21] H. Knudsen, H.-P. E. Kristiansen, H. D. Thomsen, U. I. Uggerhøj, T. Ichioka, S. P. Møller, C. A. Hunniford, R. W. McCullough, M. Charlton, N. Kuroda, Y. Nagata, H. A. Torii, Y. Yamazaki, H. Imao, H. H. Andersen, and K. Tökési, *Phys. Rev. Lett.* **101**, 043201 (2008).
- [22] S. Borbély, J. Feist, K. Tökési, S. Nagele, L. Nagy, and J. Burgdörfer, *Phys. Rev. A* **90**, 052706 (2014).
- [23] X. Guan and K. Bartschat, *Phys. Rev. Lett.* **103**, 213201 (2009).
- [24] H. Knudsen, H.-P. Kristiansen, H. Thomsen, U. Uggerhøj, T. Ichioka, S. Møller, C. Hunniford, R. McCullough, M. Charlton, N. Kuroda, Y. Nagata, H. Torii, Y. Yamazaki, H. Imao, H. Andersen, and K. Tökési, *Nucl. Instrum. Methods Phys. Res., Sect. B* **267**, 244 (2009).
- [25] A. Niehaus, *J. Phys. B: At. Mol. Phys.* **19**, 2925 (1986).
- [26] H. Cederquist, *Phys. Rev. A* **43**, 2306 (1991).
- [27] W. Eberhardt, S. Bernstorff, H. W. Jochims, S. B. Whitfield, and B. Crasemann, *Phys. Rev. A* **38**, 3808 (1988).
- [28] B. Ding, D. Yu, F. Ruan, R. Lu, C. Shao, C. Wan, S. Chen, and X. Cai, *Phys. Rev. A* **82**, 032703 (2010).
- [29] L. Végh and J. Burgdörfer, *Phys. Rev. A* **42**, 655 (1990).
- [30] J. H. McGuire, *Phys. Rev. Lett.* **49**, 1153 (1982).
- [31] F. W. Byron and C. J. Joachain, *Phys. Rev. Lett.* **16**, 1139 (1966).
- [32] T. Schneider, P. L. Chocian, and J.-M. Rost, *Phys. Rev. Lett.* **89**, 073002 (2002).
- [33] F. Zhou, Y. Ma, and Y. Qu, *Phys. Rev. A* **93**, 060501(R) (2016).
- [34] Y. Ma, L. Liu, Y. Wu, Y. Qu, and J. Wang, *Phys. Rev. A* **101**, 052703 (2020).
- [35] Note that we have also used the Dyson model approach for neon as a target and found good agreement with previous results. A paper reporting these results will be published later.
- [36] L. H. Andersen, P. Hvelplund, H. Knudsen, S. P. Møller, J. O. P. Pedersen, S. Tang-Petersen, E. Uggerhøj, K. Elsener, and E. Morenzoni, *J. Phys. B: At., Mol. Opt. Phys.* **23**, L395 (1990).
- [37] H. Knudsen, H. A. Torii, M. Charlton, Y. Enomoto, I. Georgescu, C. A. Hunniford, C. H. Kim, Y. Kanai, H.-P. E. Kristiansen, N. Kuroda, M. D. Lund, R. W. McCullough, K. Tökési, U. I. Uggerhøj, and Y. Yamazaki, *Phys. Rev. Lett.* **105**, 213201 (2010).
- [38] M. S. Pindzola, T. G. Lee, and J. Colgan, *J. Phys. B: At., Mol. Opt. Phys.* **47**, 185202 (2014).
- [39] I. B. Abdurakhmanov, A. S. Kadyrov, D. V. Fursa, and I. Bray, *Phys. Rev. Lett.* **111**, 173201 (2013).
- [40] I. B. Abdurakhmanov, A. S. Kadyrov, D. V. Fursa, S. K. Avazbaev, and I. Bray, *Phys. Rev. A* **89**, 042706 (2014).